ness of sites and the probable location of one of the sites in a zone of elastic strain accumulation.
59. K. L. Feigl, R. W. King, T. H. Jordan, *J. Geophys. Res.* **95**, 2679 (1990).
60. For example, J. Savage, *ibid.* **83**, 5487 (1978).
61. M. Lisowski, J. C. Savage, W. H. Prescott, *ibid.* **96**, 8369 (1991).
62. Such as in the tectonically stable portion of North America, that is, mainly east of the Rocky Mountains as in (*56*) also see (*49, 57*).
63. J. F. Engeln and S. Stein, *Earth Planet. Sci. Lett.* **68**, 259 (1984); J. F. Engeln, S. Stein, J. Werner, R. Gordon, *J. Geophys. Res.* **93**, 2839 (1988); R. C. Searle *et al.*, *Nature* **341**, 701 (1989).
64. G. D. Acton, S. Stein, J. F. Engeln, *Tectonics* **10**, 501 (1991); P. Tapponnier, R. Armijo, I. Manighetti, V. Courtillot, *Geophys. Res. Lett.* **17**, 1 (1990).
65. For example, M. E. Beck, Jr., *Am. J. Sci.* **276**, 694 (1976); R. W. Simpson and A. Cox, *Geology* **5**, 585 (1977); B. P. Luyendyk, M. J. Kamerling, R. R. Terres, J. S. Hornafius, *J. Geophys. Res.* **90**, 12454 (1985).
66. D. S. Caprette, C. Ma, J. W. Ryan, *NASA Tech. Memo 100765* (1990).
67. W. M. Elsasser, in *The Application of Modern Physics to the Earth and Planetary Interiors*, S. K. Runcorn, Ed. (Wiley, New York, 1969), pp. 223–246.
68. K. Shimazaki, *Phys. Earth Planet. Inter.* **8**, 148 (1974).
69. D. McKenzie and J. Jackson, *Earth Planet. Sci. Lett.* **65**, 182 (1983).
70. J. B. Minster and T. H. Jordan, in *Tectonics and Sedimentation Along the California Margin*, J. K. Crouch and S. B. Bachman, Eds. (Pacific Section, Society of Economic Paleontologists and Mineralogists, Los Angeles, 1984), vol. 38, pp. 1–16.
71. J. Jackson and D. McKenzie, *Geophys. J. R. Astron. Soc.* **93**, 45 (1988).
72. See, for example, the following review paper: W. Hamilton, *Geol. Soc. Am. Bull.* **100**, 1503 (1988).
73. For example, M. Bevis *et al.*, *Eos* **72**, 115 (1991).
74. See, for example (*61*).
75. The angular velocity is described by a right-handed rotation of 0.61° per million years about 32°N, 128°W, as documented in (*52*).
76. T. H. Jordan and J. B. Minster, in *The Impact of VLBI on Astrophysics and Geophysics, International Astronomical Union Symposium No. 129*, M. J. Reid and J. M. Moran, Eds. (Kluwer Academic, Boston, 1988).
77. R. G. Gordon, S. Stein, C. DeMets, D. F. Argus, *Geophys. Res. Lett.* **14**, 587 (1987).
78. R. G. Gordon and C. DeMets, *J. Geophys. Res.* **94**, 5560 (1989).
79. P. Tapponnier and P. Molnar, *Nature* **294**, 319 (1976); P. Bird and K. Piper, *Phys. Earth Planet. Inter.* **21**, 158 (1980); P. C. England and D. P. McKenzie, *Geophys. J. R. Astron. Soc.* **70**, 295 (1982); J. P. Vilotte, M. Daignieres, R. Madariaga, *J. Geophys. Res.* **87**, 10,709 (1982).
80. P. Molnar, in *Earthquake Mechanics, Rock Deformation, and Transport Properties of Rocks: A Festscrift in Honor of W. F. Brace*, B. Evans and T.-F. Wong, Eds. (Academic Press, London, in press); W.-P. Chen and P. Molnar, *J. Geophys. Res.* **88**, 4183–4214 (1983).
81. The plate boundaries are mainly from (*82*) with the addition of the Scotia plate (*35*) and with a few boundaries refined.
82. D. F. Argus and R. G. Gordon, *Geophys. Res. Lett.* **18**, 2038 (1991).
83. R. K. Dokka and C. J. Travis, *ibid.* **17**, 1323 (1990); J. C. Savage, M. Lisowski, W. H. Prescott, *ibid.*, p. 2113.
84. This research was supported by National Science Foundation grant OCE-8900090 and National Aeronautics and Space Administration grant NAG5-885. We thank S. Agar, B. Cameron, and two anonymous reviewers for rapid and helpful reviews. The outlines of the idealized narrow plate boundaries and of the wide plate boundary zones shown in Fig. 1 incorporate several improvements made by T. Shoberg, who also prepared both Figs. 1 and 2.

Measured Trends in Stratospheric Ozone

Richard Stolarski, Rumen Bojkov, Lane Bishop, Christos Zerefos, Johannes Staehelin, Joseph Zawodny

Recent findings, based on both ground-based and satellite measurements, have established that there has been an apparent downward trend in the total column amount of ozone over mid-latitude areas of the Northern Hemisphere in all seasons. Measurements of the altitude profile of the change in the ozone concentration have established that decreases are taking place in the lower stratosphere in the region of highest ozone concentration. Analysis of updated ozone records, through March of 1991, including 29 stations in the former Soviet Union, and analysis of independently calibrated satellite data records from the Total Ozone Mapping Spectrometer and Stratospheric Aerosol and Gas Experiment instruments confirm many of the findings originally derived from the Dobson record concerning northern mid-latitude changes in ozone. The data from many instruments now provide a fairly consistent picture of the change that has occurred in stratospheric ozone levels.

Ozone is continuously being produced in the stratosphere by solar ultraviolet radiation. Radiation at wavelengths less than 242 nm dissociates molecular oxygen into atoms that attach themselves to O_2 to form ozone. The destruction of ozone in the stratosphere is dominated by the catalytic reactions of the nitrogen, hydrogen, chlorine, and bromine oxides. The ozone concentration peaks in the stratosphere at an altitude of 20 to 25 km. The distribution of ozone is maintained by a balance between its production and loss and by the transport of ozone from regions of net production to those of net loss. The transport of ozone is driven by the variable wind fields of the stratosphere, which give rise to daily fluctuations, seasonal variations, and interannual variability in ozone amounts.

Starting in the early 1970s, predictions have been made that human activities will lead to a diminishing of the earth's protective ozone layer (*1*). The search for evidence of downward trends in the thickness of the ozone layer was inconclusive until the discovery of the Antarctic ozone hole in 1985 (*2*). Ozone decreases during the Antarctic spring are now well documented (*3*). Ozone decreases outside the Antarctic, at southern mid-latitudes, have been reported, as well as over the heavily populated northern mid-latitudes (*4*).

Assessments of the state of knowledge about ozone depletion have been published in various joint reports from the World Meteorological Organization and the United Nations Environment Program. In this paper, based on a chapter of the most recent report (*5*), we review the evidence for ozone depletion and analyze some of the updated records.

R. Stolarski is at the Goddard Space Flight Center, Greenbelt, MD, 20771. R. Bojkov is at the World Meteorological Organization, Geneva 20, Switzerland 1211. L. Bishop is at Allied Signal, Buffalo, NY 14210. C. Zerefos is at the University of Thessaloniki, Thessaloniki, Greece 54006. J. Staehelin is at the Laboratory for Atmospheric Physics, ETH, 8093 Zurich, Switzerland. J. Zawodny is at the Langley Research Center, Hampton, VA 23665.

Sources of Data

Ozone measurements can be divided into two important types: those that measure the total thickness of the ozone layer and those that measure the ozone concentration as a function of altitude. Historically, the most important instrument for the measurement of the total thickness of the ozone layer has been the Dobson spectrophotometer, designed in the 1920s and still in use today. The Dobson instrument, located on the ground, measures the solar radiation transmitted through the ozone layer at pairs of wavelengths near 300 nm. One wavelength is chosen so that it is significantly absorbed by ozone while the other is attenuated in the instrument by a calibrated optical wedge. The wedge position is adjusted until equal signals for the two beams are obtained. Measurements are made for two separate pairs of wavelengths to allow cancellation of errors due to aerosols in the atmosphere (*6*).

Daily measurements have been made using a Dobson instrument at the station in Arosa, Switzerland, from 1926 to the present. Since 1957, a network of more than 30 stations has been making measurements of the total ozone thickness. This network is spread over much of the world but is heavily concentrated in the Northern Hemisphere (*7*). The network of instruments is calibrated relative to a single "world standard instrument," which is itself calibrated each summer at Mauna Loa. The calibration is then transferred to the rest of the instruments through secondary standards (8).

The data from the worldwide network of ozone-measuring stations are reported to the World Ozone Data Center in Toronto and are published monthly (9). The data reported are those by each station, generally with the use of the latest calibration. The records have not always been entirely consistent, however, and the Ozone Trends Panel (10) used data from Dobson stations that had been provisionally revised by Bojkov using monthly mean corrections (11). Since then a number of the Dobson stations have revised their entire data records, making daily corrections based on detailed calibration records. These include Belsk, Hradec Kralove, Ahmedabad, and the four Japanese stations: Sapporo, Tateno, Kagoshima, and Naha. Several other stations have been provisionally revised on a monthly basis by the station. We use Bojkov's provisional revisions for the rest of the stations in our analysis. All data that we use have been updated through March of 1991.

Another instrument used for making total ozone column measurements from the ground is the filter ozonometer. This instrument, called the M83, was developed in the mid-1950s. In its initial configuration, the instrument had significant systematic errors. In the early 1970s the instrument was modified and improved by implementing narrower band light filters. Since 1973 this modified instrument has been used at 45 ozone monitoring stations located in the former Soviet Union. Since 1986 the M83 has been replaced by the M124, which is a modified design with the same light filters. The data before 1973 should not be used for the analysis of trends because of large systematic errors. One cause of the instrument problems was the frequent replacement of instruments with new ones about every 2 years. We use data from this network that have been revised by careful checking of calibration records at each station (12).

Since November of 1978, total ozone has been measured on a nearly global basis by the Total Ozone Mapping Spectrometer (TOMS) from the Nimbus 7 satellite. TOMS measures the earth's ultraviolet albedo at several wavelengths near 300 nm. The main problem with maintaining a long-term ozone record with TOMS has been the degradation of the diffuser plate used to make the solar observation for determination of albedo. Early evaluations of the ozone data from TOMS (13) included a correction for darkening of the diffuser plate. This correction yielded a TOMS data set that tracked the corresponding Dobson measurements until about 1982 or 1983. After that the TOMS, and the companion SBUV instrument, began to drift downward with respect to Dobson measurements (10). A new method has been recently derived to improve the correction to the diffuser plate (14). The entire data set has now been reprocessed and is estimated to be precise to ±1.3% (2σ) at the end of 1989 relative to the beginning of the record.

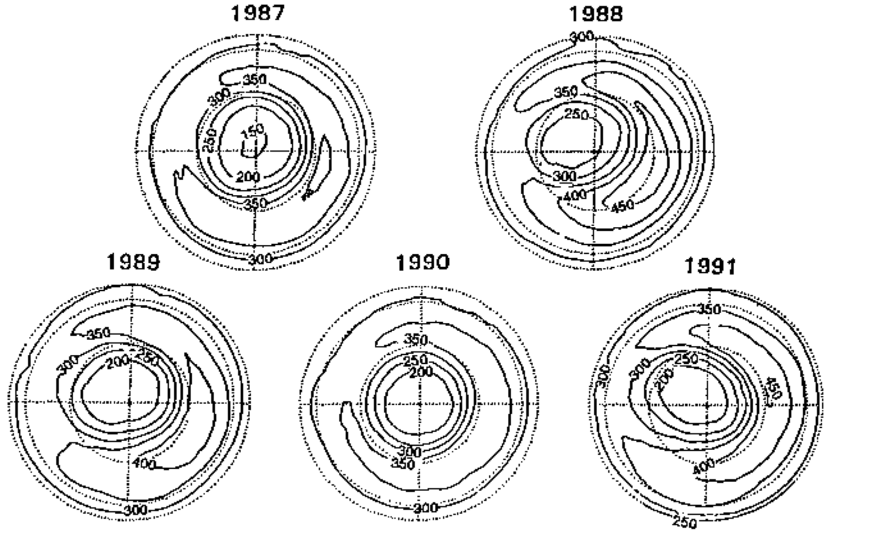

Fig. 1. Polar orthographic projections of TOMS Southern Hemisphere maps of October mean total ozone for each of the last 5 years. The South Pole is at the center; the equator, 30°S, and 60°S latitude circles are shown; and Greenwich is to the top. The contours are in Dobson units.

Earlier assessments of the change in the altitude profile of the ozone concentration included analysis of data through 1986 from a network of nine ozonesonde stations (15). The sondes are balloon-launched electrochemical sondes that measure ozone from the ground to about 30 km altitude (16). The data from these stations have been recently updated and reanalyzed (17). There has been no updated trend analysis of the overall network, but we use the record from Payerne, Switzerland (18), to illustrate some of the features of the observed profile of ozone loss.

The Umkehr technique for measuring the profile of ozone concentration has been in use since its discovery by Götz (19). It consists of observing the zenith sky radiance as the sun sets at the ozone-absorbing wavelengths used in Dobson total ozone measurements. Information about the profile is obtained from an inversion algorithm applied to the data. Mateer and DeLuisi have devised an improved Umkehr retrieval algorithm (20). With the use of this algorithm and a correction for the interference of the aerosol from the El Chichon volcanic eruption, the Umkehr record for the past 12 years for ten stations has been reassessed (21).

Satellite measurements of the vertical profile of stratospheric ozone have been made by the Stratospheric Aerosol and Gas Experiment (SAGE). SAGE I data began in February 1979 and extend through November 1981. SAGE II began operation in October 1984 and continues to make measurements today. The SAGE technique is solar occultation, and profile measurements are obtained at sunrise and sunset on each orbit (22). This measurement technique is insensitive to drift in instrumental calibration; however, there may be systematic differences between the data from SAGE I and SAGE II. The potential systematic differences are less than 2% between 25 and 45 km but increase to approximately 6% at 20 km. The largest improvement from earlier assessments is that the SAGE I and II ozone profiles below 25 km have now been extensively intercompared with data from ozone sondes, and trend estimates can be made down to 17 km altitude (23).

Antarctic Ozone Update

The springtime Antarctic ozone hole was discovered in 1985 but is observable in data since about the late 1970s (2). Measurements by ground-based instruments, balloonsondes, and satellites have shown that the depletion occurs mainly during September. In recent years the ozone concentration in the lower stratosphere between about 14 and 22 km declined to near zero by early October (24).

In both 1989 and 1990, the Antarctic ozone hole was characterized by low total ozone values over much of the south polar region (25). The depth and extent of the hole in each of these years were comparable to the large 1987 ozone hole (Fig. 1). In 1990, the hole lasted a particularly long time, until the polar vortex broke down in late December. The vortex appeared to have been weakened by wave events in August, but it persisted because the wave activity that was propagated upward from the troposphere also weakened. The 1991

TOMS total ozone data (26) show a decline through early October that is similar to the earlier deep ozone hole years 1987, 1989, and 1990. A minimum value of 108 Dobson units (DU), slightly lower than in earlier years, was reached in early October 1991. The recovery through the middle of November 1991 has closely followed that of 1989. The quasi-biennial modulation of the depth of the ozone hole, which has been previously noted (27), is not evident in the data for the last 3 years (Fig. 1).

The September decrease in Antarctic ozone has been clearly shown to be a lower stratospheric phenomenon (mainly between 14 and 22 km altitude). Nearly all of the ozone was removed in cold years with deep ozone holes (24). This was again the

Table 1. Long-term trends derived from ground-based total ozone data for individual stations. These estimates were derived from the Allied-Signal statistical model using data from January 1958 through March 1991 where possible, with a linear trend fit to the period 1970 to 1991. Right-side columns show a comparison of TOMS ozone trends with short-term trends (over the same data period, November 1978 to March 1991) derived from ground-based total ozone data for individual stations. The TOMS trends given in the table are calculated for the 5° latitude by 10° longitude block containing the station. Lat, latitude; SE, standard error.

	Lat	Long-term trends								Code*	Short-term trends							
											December–March				May–August			
		Year-round		Dec–Mar		May–Aug		Sep–Nov			Ground		TOMS		Ground		TOMS	
		Trend	SE	Trend	SE	Trend	SE	Trend	SE		Trend	SE	Trend	SE	Trend	SE	Trend	SE
North America																		
Churchill	59 N	−3.4	0.5	−4.3	0.8	−3.2	0.6	−2.4	0.8	2	−5.4	2.3	−2.3	2.1	−6.7	1.5	−6.4	1.5
Edmonton	54 N	−1.4	0.4	−2.6	0.8	−0.7	0.6	−0.4	0.7	2	−5.5	2.1	−5.5	2.2	−7.5	1.0	−5.2	1.2
Goose Bay	53 N	−1.3	0.4	−1.4	0.8	−1.5	0.5	0.1	0.6	2	2.1	2.6	−1.1	2.4	−5.1	1.4	−4.3	1.3
Caribou	47 N	−2.2	0.4	−3.7	0.8	−1.2	0.4	−1.1	0.6	2	−4.7	2.4	−3.5	2.6	−3.4	1.1	−4.3	1.2
Bismarck	47 N	−2.4	0.4	−3.5	0.7	−2.0	0.5	−1.0	0.6	2	−4.4	1.9	−4.6	1.8	−5.1	1.4	−5.2	1.3
Toronto	44 N	−1.5	0.4	−3.1	0.8	−1.3	0.4	0.1	0.7	2	−4.3	2.0	−6.6	2.4	−2.8	1.1	−3.1	0.9
Boulder	40 N	−2.7	0.4	−3.1	0.8	−2.6	0.4	−1.8	0.6	2	−2.4	2.0	−4.4	1.9	−2.5	1.2	−3.6	1.2
Wallops Island	38 N	−1.5	0.6	−2.9	1.2	−0.8	0.7	−1.3	0.8	2	−6.8	1.8	−7.4	2.1	−1.9	1.6	−2.6	1.0
Nashville	36 N	−2.1	0.4	−3.3	0.8	−2.0	0.4	−1.6	0.6	2	−7.3	1.9	−6.8	2.1	−2.0	1.2	−1.8	0.9
Tallahassee	30 N	−2.0	0.5	−3.5	0.9	−1.5	0.5	−1.7	0.6	3	−5.8	2.8	−6.3	1.9	−2.8	2.0	−1.7	0.9
Simple average		−2.1		−3.1		−1.7		−1.1			−4.5		−4.8		−4.0		−3.8	
Europe																		
Reykjavik	64 N	−0.3	0.7	0.2	1.4	−0.7	0.6	−0.2	1.1	3	0.0	5.6	−0.8	4.1	−4.8	1.3	−4.5	1.4
Lerwick	60 N	−0.1	0.7	0.9	1.5	−1.0	0.6	0.7	1.1	1,2	1.3	13.7	−2.9	3.6	−5.6	1.9	−5.7	1.5
St. Petersburg	60 N	−3.1	0.5	−4.5	1.1	−1.8	0.6	−2.5	0.8	2	−4.6	2.7	−5.8	2.6	−4.0	1.6	−4.7	1.4
Belsk	52 N	−2.2	0.5	−3.8	1.0	−1.0	0.6	−1.6	0.8	1	−5.4	2.8	−5.9	2.9	−5.3	1.3	−4.1	1.6
Bracknell	51 N	−3.4	0.5	−4.3	1.0	−3.1	0.6	−2.3	0.9	1,2	−3.8	2.5	−4.4	2.7	−5.9	1.3	−5.0	1.4
Hradec Kralove	50 N	−1.8	0.5	−4.0	0.9	−0.3	0.5	−0.7	0.7	1	−5.0	2.6	−6.6	2.6	−3.5	1.1	−4.4	1.4
Uccle	51 N	−2.9	0.6	−2.5	1.3	−2.7	0.7	−3.4	1.1	3	−4.4	2.7	−6.3	2.6	−4.3	1.3	−4.7	1.3
Hohenpeissenberg	48 N	−2.3	0.5	−3.1	1.0	−1.7	0.5	−1.2	0.8	1,2	−3.8	2.9	−6.9	2.7	−2.4	1.1	−3.7	1.2
Arosa	47 N	−2.4	0.4	−3.4	0.8	−1.8	0.4	−1.8	0.6	2	−5.9	2.5	−6.1	2.7	−2.8	1.3	−4.4	1.4
Vigna di Valle	42 N	−0.8	0.4	−2.3	0.9	0.4	0.5	−0.2	0.5	2	−6.0	2.8	−6.3	2.5	−4.4	1.3	−3.4	1.1
Cagliari/Elmas	39 N	−0.4	0.5	−1.8	1.0	0.7	0.6	−0.1	0.8	2	−3.8	3.4	−4.4	2.5	−0.8	2.3	−2.7	1.2
Simple average		−1.9		−2.9		−1.2		−1.3			−3.8		−5.1		−4.0		−4.3	
Far East																		
Nagaevo†	60 N	−3.4	1.0	−2.5	1.9	−4.6	1.2	−0.8	2.0	1,2	−4.3	2.5	−4.4	2.1	−3.0	2.0	−3.9	1.5
Petropavlosk†	53 N	−2.4	0.8	−2.0	1.4	−1.8	1.6	−3.0	1.1	1,2	−5.2	2.1	−6.8	1.7	−1.8	2.7	−3.8	1.5
Sahalin†	47 N	−2.0	0.8	−2.7	1.4	−0.9	1.2	−2.4	1.1	1,2	−4.2	1.5	−7.6	1.5	−1.1	1.7	−4.3	1.5
Sapporo	43 N	−1.3	0.5	−2.4	0.8	−1.1	0.6	−0.2	0.6	1	−3.7	2.1	−6.8	2.1	−4.0	1.6	−3.9	1.7
Tateno	36 N	−0.9	0.4	−2.1	0.8	−0.6	0.4	0.3	0.5	1	−3.3	2.3	−6.2	2.2	−2.2	1.2	−3.3	1.2
Kagoshima	32 N	0.4	0.5	−0.4	0.8	0.7	0.5	1.0	0.6	1	−2.9	1.9	−5.0	2.0	−1.5	1.1	−2.6	1.1
Naha	26 N	−0.3	0.7	−0.8	1.2	−0.1	0.8	−0.3	0.9	1	−3.2	1.8	−3.5	1.6	−1.3	1.1	−2.2	1.0
Simple average		−1.5		−2.0		−1.2		−0.8			−3.8		−5.8		−2.1		−3.4	
Low latitude																		
Quetta	30 N	−0.2	0.6	−0.1	0.9	0.2	0.6	−0.4	0.7	2	−3.0	2.6	−4.8	2.4	−0.9	1.5	−2.6	1.3
Cairo	30 N	0.0	0.8	−0.5	1.7	−0.4	0.9	1.0	0.8	2	−1.6	2.5	−3.2	2.2	−1.2	1.2	−3.0	1.0
Ahmedabad	23 N	0.4	0.5	−0.7	0.8	1.0	0.7	1.3	0.6	1	−0.3	2.4	−2.3	1.6	−2.3	1.5	−0.9	1.0
Mauna Loa	20 N	−0.2	0.5	−0.8	0.8	0.3	0.5	−0.4	0.5	2	1.0	2.3	−1.8	2.1	2.0	1.4	0.3	1.0
Mexico City	19 N	1.6	1.3	1.7	2.3	0.7	1.7	2.1	0.8	3	3.8	4.8	−1.8	1.8	3.7	4.0	0.1	1.1
Huancayo	12 S	−0.5	0.2	−0.7	0.3	−0.6	0.3	−0.2	0.3	2	1.2	0.6	0.1	0.6	−0.5	0.8	−0.3	0.9
Samoa	14 S	−1.2	1.0	−1.8	0.9	1.8	1.5	0.4	1.4	2	−0.4	1.1	−1.1	1.1	0.5	2.0	−1.1	1.5
Simple average		−0.2		−0.6		+0.2		+0.4			+0.1		−2.1		+0.2		−1.1	
Southern Hemisphere																		
Aspendale	38 S	−2.6	0.4	−3.1	0.4	−2.5	0.6	−2.3	0.6	1,2	−4.6	1.0	−3.2	0.9	−2.9	1.4	−3.0	1.7
Hobart	43 S	−2.2	0.4	−1.6	0.6	−3.4	0.6	−1.2	0.7	2	−5.5	1.3	−3.7	1.0	−5.5	1.6	−4.8	1.7
Invercargill	46 S	−3.5	0.5	−3.8	0.7	−3.8	0.8	−2.7	0.9	1	−7.1	1.4	−5.0	1.0	−6.1	1.7	−6.6	1.9
MacQuarie Island	54 S	−0.1	0.8	1.0	1.0	−1.2	1.1	0.1	1.3	3	−6.1	2.1	−5.9	1.1	−4.5	2.8	−5.8	2.1
Simple average		−1.1		−1.1		−1.1		−0.4			−5.8		−4.5		−4.8		−5.0	
Overall average		−1.5		−2.1		−1.2		−0.8			−3.5		−4.6		−3.0		−3.5	

*Codes: 1, reevaluated by the operating agency; 2, provisionally reevaluated (R. Bojkov); 3, needs further reevaluation. †M83 stations.

case in 1989 and 1990 (*25*). The lower stratospheric ozone decrease detected by balloon ozonesondes has been confirmed by measurements from SAGE (*28*), from lidar (*29*) and from in situ measurements on aircraft (*30*).

A measure of the size of the ozone hole is the area for which the TOMS total ozone measurements are less than 200 DU. By this measure, the size of the ozone hole reached a maximum of about 14 million square kilometers, or approximately the size of the Antarctic continent, for each of the four recent years with deep ozone holes (1987, 1989, 1990, and 1991) (*26*). In 1988, the area reached a maximum of only 5 million square kilometers.

Another measure of the ozone hole can be obtained from the monthly mean TOMS measurements for the month of October. In October 1991, the lowest monthly mean was just over 150 DU offset from the pole (Fig. 1). A strong maximum of ~450 DU was observed over the southern Indian Ocean. The pattern was similar to that of 1989. In contrast, the hole in 1987 and 1990 was more symmetric about the South Pole. Averaged over the month of October, the 1987 ozone hole had the lowest measured ozone amounts, <150-DU region around the pole, of any year so far.

Total Ozone Trends from Ground Stations

As in earlier reports (*10, 15*) we used a statistical model for the trend analysis of ozone time series. The model fits terms for seasonal variation in mean ozone, seasonal variation in ozone trends, and the effects of the quasi-biennial oscillation (QBO), solar cycles, atmospheric nuclear tests (where appropriate), and autocorrelated noise (*15, 31*). For the longer Dobson series, the trend fitted for each month is in the shape of a "hockey stick," with a level base line before December 1969 and a linear trend after 1970. For series that began after 1970, the trend is a simple linear monthly trend.

We performed two different types of analysis on the ground-based data. The standard analysis was a trend analysis at each ground-based station. Results were calculated for the seasons December to March (Northern Hemisphere winter), May to August (Northern Hemisphere summer), September to November (Northern Hemisphere fall), and a year-round trend, which is the average trend over all months of the year (Table 1). As a continuation of this form of analysis, individual station trends can be appropriately averaged over regions to yield regional trends, as reported in Table 2 for North America, Europe, and the Far East.

The second type of analysis was to form a composite ozone series for a region by a combination of the individual ozone series at the stations in that region. The primary advantage of this approach is the ability to include data from stations with records too short to analyze with the normal trend analysis, or stations that stopped taking data before the beginning of the trend period, in order to stabilize the regional or belt average. In the case of the filter (M83 or M124) data, the ozone records are so variable that regional averages supply considerable stabilization. The method of producing these series was to average the deseasonalized series together and then to add back in an average seasonal component in order to calculate percentage trends. A problem with this construction is that series with data starting after the beginning of the trend period (usually taken to be 1970) are adjusted to have monthly means of zero, and this has the effect of muting any negative trend in the composite series when a late-starting series is averaged in with the rest. Other methods of seasonal adjustment have been investigated, but no completely satisfactory technique has been found. Trends from the zonal series appear to be sensitive to the method of composition of the aggregate series, and these will be used

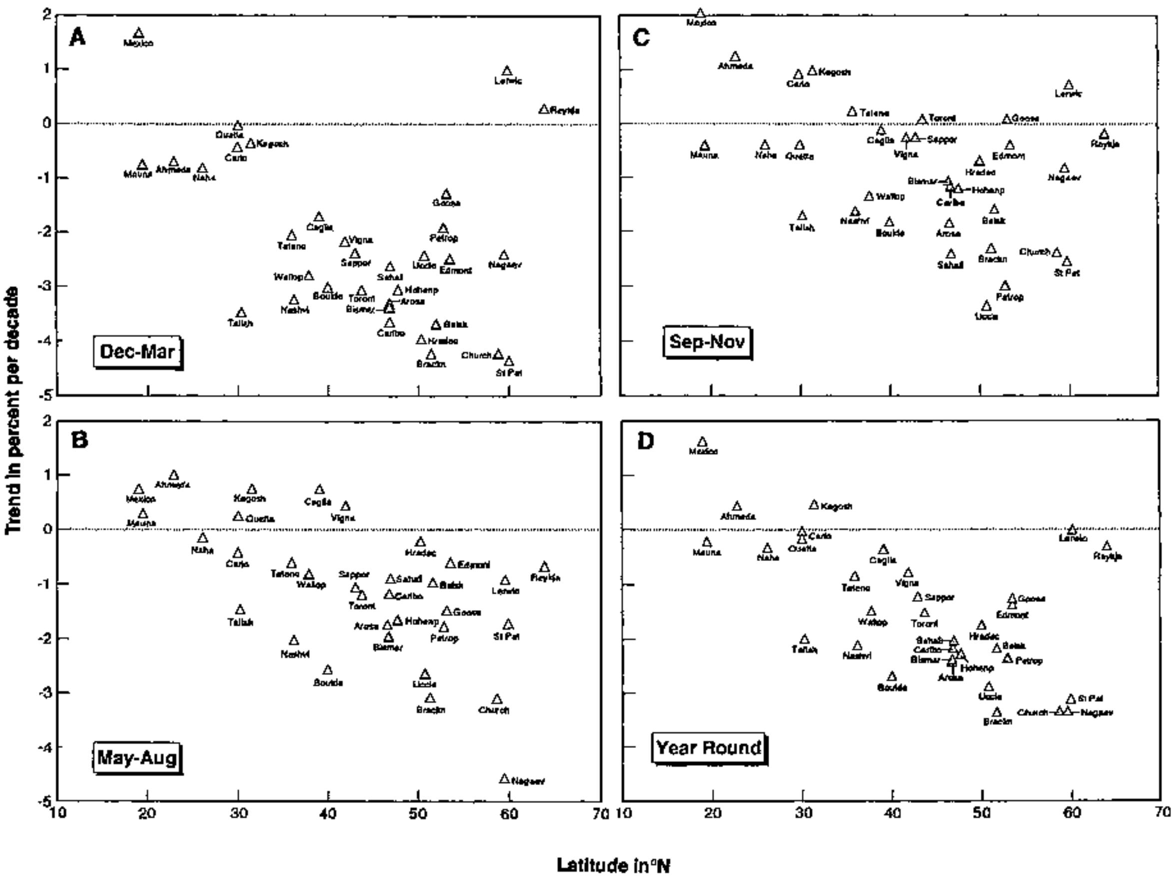

Fig. 2. Individual station long-term trends, by season, for 39 Northern Hemisphere stations, versus station latitude. The estimates were derived from the standard seasonal model using data from 1958 through 1969 as a base line and monthly linear trends over the period 1970 through March 1991.

for illustration and sensitivity studies only. However, trends obtained from the composite filter series are not very sensitive to the method of construction because the individual series have a common time span.

As shown in Table 1 and Fig. 2, ozone amounts have declined since 1970 over nearly all northern mid-latitude stations in all seasons and year-round. There is also a clear gradient with latitude in that more northerly stations exhibit the largest negative trends. The two most northerly stations, Reykjavik and Lerwick, break the pattern, however. Ozone amounts have evidently increased in winter, and either increased slightly or remained constant in summer over these two stations. This pattern may reflect difficulty in measuring ozone at low sun angles or may be an indication of longitudinal variation in ozone trends. We discuss these possibilities further below in conjunction with the TOMS data analysis.

We calculated average trends, since 1970, over North America, Europe, and the Far East using a variance-components model (32), which takes into account the precision of the trend estimate at each station (primarily length of record and natural variability) and variability of the station trends inside a region. The average of these regional trends, presented in Table 2 as the 26° to 64°N combined Dobson trend, is −2.7% per decade in the winter, −1.3% per decade in the summer, and −1.0% per decade in the fall. All of these declines are statistically significant.

Table 2. Regional and zonal long-term ozone trends derived from ground-based total ozone data. These estimates were derived in a similar manner to those in Table 1.

Region	Year-round		Dec–Mar		May–Aug		Sep–Nov	
	Trend	SE	Trend	SE	Trend	SE	Trend	SE
Dobson regional trends								
North America	−2.1	0.3	−3.2	0.4	−1.7	0.4	−1.1	0.3
Europe	−1.8	0.3	−2.9	0.4	−1.2	0.3	−1.2	0.3
Far East*	−1.2	0.4	−1.8	0.5	−0.9	0.5	−0.4	0.4
26° to 64°N combined	−1.8	0.2	−2.7	0.3	−1.3	0.2	−1.0	0.2
Filter (M83/124) regional trends								
Central Asia	−1.4	0.6	−2.1	1.1	−0.7	0.8	−1.8	0.7
Eastern Siberia	−2.1	0.6	−2.2	1.2	−1.0	0.7	−2.2	0.6
European region	−3.2	0.6	−4.1	1.2	−2.5	0.7	−2.1	0.5
Western Siberia	−1.6	0.6	−1.9	1.3	−1.0	0.6	−1.6	0.7
Average filter	−2.1	0.3*	−2.6	0.6*	−1.3	0.4†	−1.9	0.3†
Combined regional	−1.8	0.3	−2.7	0.4	−1.3	0.2	−1.2	0.3

*Includes three filter stations. †Estimated standard error, not calculated.

Although a significant decline in winter had been identified, our analysis yields a winter decline that is slightly greater than earlier estimates (10, 11, 15). The earlier assessments concluded that ozone amounts during summer had not changed significantly (fall trends were not given). Bojkov *et al.* (11) found a (barely) significant summer decline, but the fall trend was nearly zero. Composite series for North America, Europe, and the Far East (Fig. 3) show an apparent increase in slope after 1980 that is quite noticeable for North America and Europe. This increase in the negative trend in the 1980s is discussed again later when the TOMS data are considered.

Composite series (the second method described previously) were constructed for the filter (M83 or M124) data for four major regions of the former Soviet Union where the characteristics of the ozone regime have shown some distinguishable differences (12). The trends obtained from fitting these regional series are similar to the Dobson regional results; negative trends were significant in every season. Given the close match of the Dobson and filter results, it makes sense to combine these estimates, although they derive from different instruments and different types of analyses. If we consider the former Soviet Union as a fourth region, we can compute an omnibus mid-latitude North Hemisphere trend (given in Table 2 as "combined regional trends"). The decreases in ozone estimated from this combination are −2.7% per decade in the winter, −1.3% per decade in the summer, and −1.2% per decade in the fall. All of these are statistically significant. These combined regional results are our best estimates of the overall mid-latitude Northern Hemisphere seasonal decreases in the column amount of ozone since 1970.

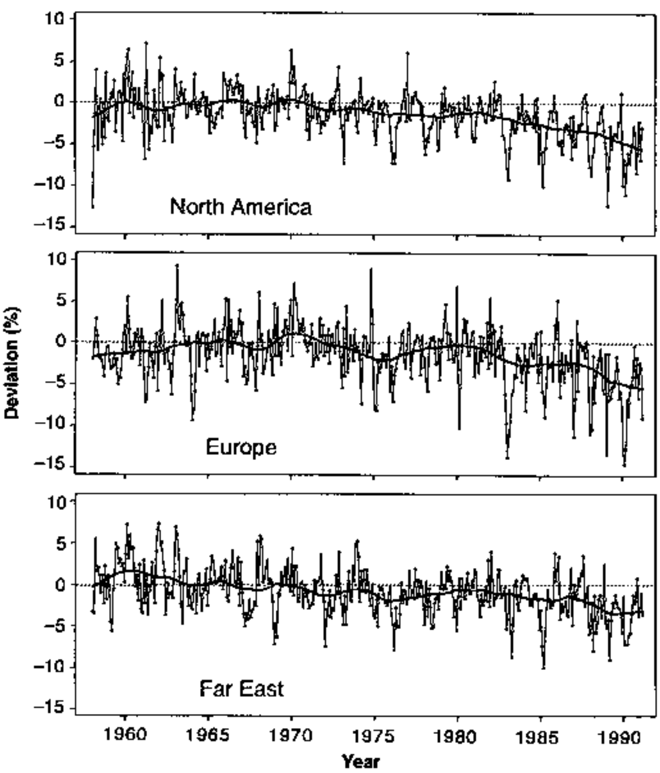

Fig. 3. Regional average ozone series versus time. The series were calculated by taking seasonal, solar, QBO, and nuclear components at each station as determined from the full standard model (including trends) and subtracting these components (but not the trend component) from the ozone series at each station. The resulting series with seasonal, solar, and so forth components removed were averaged over all stations in the respective regions. The thick line is a strong statistical smoother (a 4-year moving robust regression) intended to bring out the slowly changing features in the data.

Ground station versus satellite data. The decreases estimated above are based on a 33-year record from 1958 to 1991, whereas the satellite record is just over 12 years in length. This raises the question of interpreting the 12-year trends in the context of the longer Dobson record. Comparison of the TOMS data to the World Primary Standard Dobson Instrument (#83) when TOMS passes over that instrument during its calibration each summer at Mauna Loa shows agreement over the time period November 1978 to March 1991 to within stated error (33).

Comparison of the trend derived from TOMS over each Dobson station to the trend derived from the Dobson data for the TOMS time period shows that the trends derived from TOMS data are more negative than those derived from the Dobson data (Table 1): −4.6 versus −3.5% per decade for December to March and −3.5 versus −3.0% per decade for May to August. The recent short-term decreases derived from the Dobson data are consistently larger than those derived over the longer time period since 1970 for the non-equatorial stations (poleward of 25° north or south): trends at 30 out of 34 stations are more negative in both seasons.

Trends from Satellite Data

The TOMS data were previously analyzed for trends over the period November 1978 to May 1990 (*34*). No ozone trend was found near the equator, but an increasingly negative trend was evident toward high latitudes in both hemispheres. An update of those results through March of 1991 (Fig. 4) shows that the trends are similar to those previously reported through May of 1990. Trends are shown only to within about 10° of the terminator because of possible problems with the TOMS data at high solar zenith angles (*35*). The statistical model used to determine ozone trends included a fit to the 11-year solar cycle, the QBO, and a linear trend. The Northern Hemisphere decrease in total ozone exhibits a winter to early spring maximum located at mid-latitudes. The wintertime peak rate of ozone decrease near 40°N is slightly greater than 6% per decade, slightly less than the 8% per decade reported from data extending through May 1990 (*34*).

Because of the global coverage of the TOMS data, it can also be used to map the latitudinal and longitudinal structure of the ozone change (Fig. 5). The TOMS results for the months from December through March (Northern Hemisphere winter) show strong longitudinal variations at high northern latitudes, which are also seen in the ground-based data. The longitudinal variations at 60°N are marginally statistically significant, but there is no obvious way to determine whether they indicate a longitudinal variation in the cause of the trend. For the season May through August (Southern Hemisphere winter and Northern Hemisphere summer), longitudinal variations are seen in both hemispheres but are not as pronounced as those from December to March in the northern high latitudes (Fig. 6).

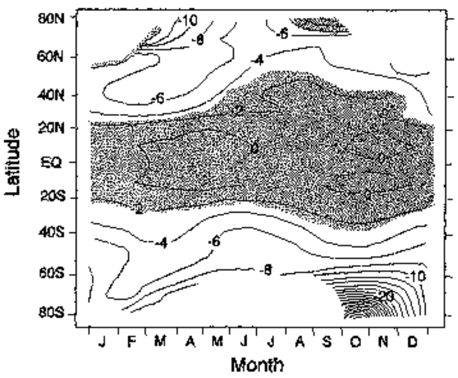

Fig. 4. Trend in percent per decade obtained from TOMS total ozone data as a function of latitude and season. Data included extend from November 1978 through March 1991. Unshaded area indicates where trends are statistically significant at the 2σ level (*38*).

Trends in the Ozone Profile

Before the discovery of the Antarctic ozone hole, model predictions of the change in column amount of ozone were about 1% per decade with the maximum expected change occurring in the upper stratosphere near 40 km. Changes in the Antarctic spring, however, were clearly shown to be occurring in the lower stratosphere, as discussed above. One would also suspect that, because mid-latitude ozone decreases have been 5% or greater (as reported above), most of the losses would be in the lower stratosphere

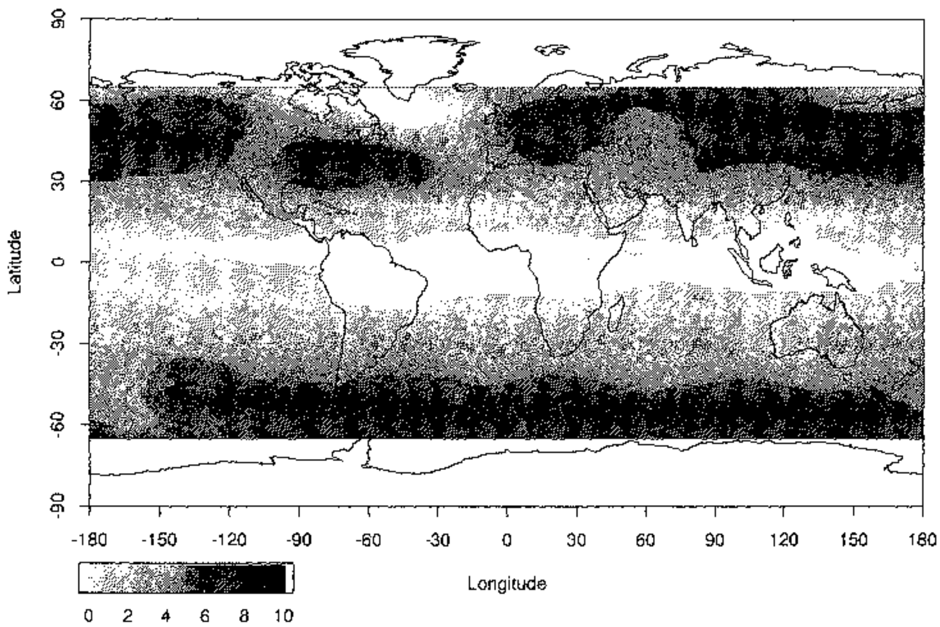

Fig. 5. Contours of constant TOMS average trends in percent per decade for December through March over the period from November 1978 through March 1991, versus latitude and longitude.

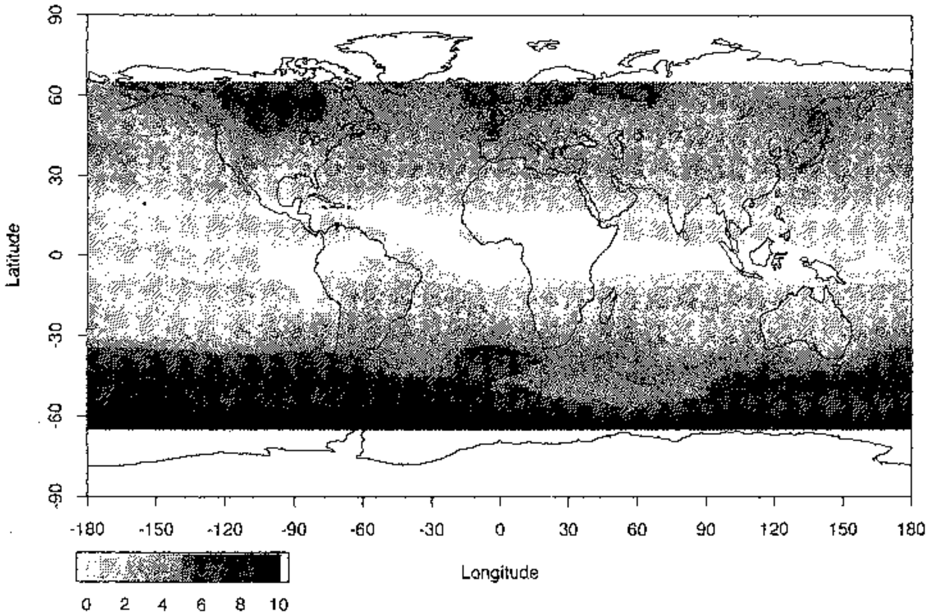

Fig. 6. Same as Fig. 5 except for the season from May through August.

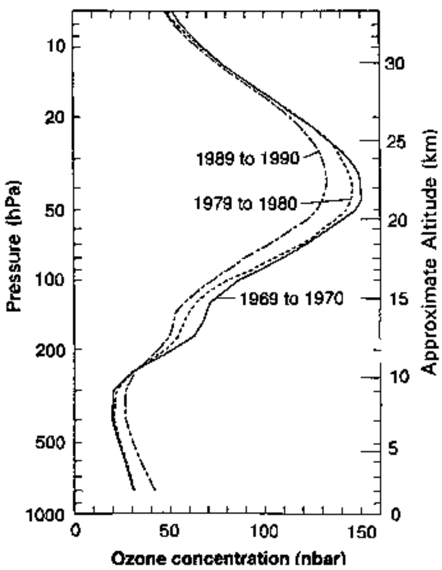

Fig. 7. Average ozone concentration versus altitude measured over Payerne, Switzerland, for three 2-year periods, 1969–1970, 1979–1980, and 1989–1990. Periods were chosen to be approximately during solar maximum and 2 years were used to remove most of any QBO effect.

where most of the ozone is located. Earlier assessments, on the basis of data through 1986, did show a statistically significant negative trend between about 17 and 24 km, but extreme caution was urged in drawing conclusions on a global scale because there were considerable differences in trend profiles from station to station (*15*).

Time series of ozone concentration measurements, made by ozonesondes at seven stations, have recently been reanalyzed to include data through 1991 (*36*). The data from each of the stations show a statistically significant increase in the ozone concentration in the troposphere and a statistically significant decrease in the ozone concentration in the lower stratosphere (Fig. 7). Tropospheric ozone increases ranged from 5 to 20% per decade whereas stratospheric decreases ranged from 5 to 15% per decade. The ozonesonde time series at Payerne, Switzerland, has recently been analyzed for each of three seasons for data from 1967 through 1990 (*18*). The increase in tropospheric ozone levels was statistically significant for each season, as was the decrease in stratospheric ozone levels. The crossover from tropospheric increases to stratospheric decreases occurred at the lowest altitude in winter (≈200 mbar) and the highest altitude in fall (≈100 mbar). Because the total ozone column from each ozonesonde profile is normalized to Dobson column measurements, the integrated effect of the sonde trend profile is necessarily quantitatively consistent with the Dobson trends.

In an earlier assessment (*10*) ozone changes as a function of altitude above 25 km were obtained by differencing 3 years of SAGE II data from the >2 years of SAGE I data. Now there are more than 6 years of SAGE II data, and the ozone profiles from both instruments have been validated below 25 km altitude (*37*), allowing the deduction of trends down to 17 km altitude.

Ozone trends deduced from the combined SAGE I and SAGE II measurements in the middle stratosphere (25 to 35 km) are small and not significantly different from zero (Fig. 8). Above 35 km, the trends are generally negative. The maximum decrease is found near 42 km at 20°S latitude, and changes in the Southern Hemisphere have been larger than those in the Northern Hemisphere. The altitude distribution of the upper stratospheric decrease is consistent with model predictions, but the magnitude deduced from SAGE measurements is significantly less than model predictions (Fig. 9). In the lower stratosphere, large decreases are deduced and the latitude dependence is weak. The largest lower stratospheric decrease appears near about 25° in each hemisphere.

Analysis of Umkehr data from ten stations (*21*) also shows upper stratospheric decreases with an altitude shape similar to that from model predictions (Fig. 9). The magnitude of the upper stratospheric decrease in ozone concentration derived from Umkehr data is larger than that derived from SAGE but still less than that predicted by models. No significant trend is observed in the region between 25 and 30 km. The SAGE, Umkehr, and ozonesonde data independently confirm that large ozone decreases have occurred in the lower stratosphere (below 25 km).

Fig. 8. Trends derived from the SAGE I and SAGE II measurements of the ozone profile in percent per decade as a function of latitude and altitude (*23*).

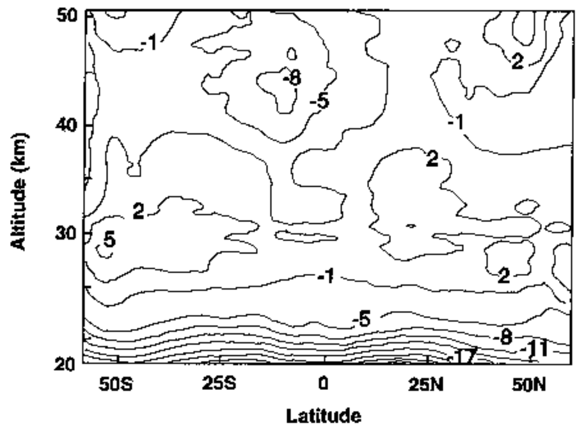

Fig. 9. Comparison of ozone profile trend estimates from several measurement systems, SAGE, Umkehr, and ozonesonde stations. SAGE data are an average of the latitudes 50°N and 50°S. The Umkehr is the average over five northern mid-latitude stations. The ozonesondes are an average over six northern mid-latitude stations. Shaded area shows the range of two model calculations at 50°N and 50°S. The panel on the right shows a typical ozone concentration versus altitude.

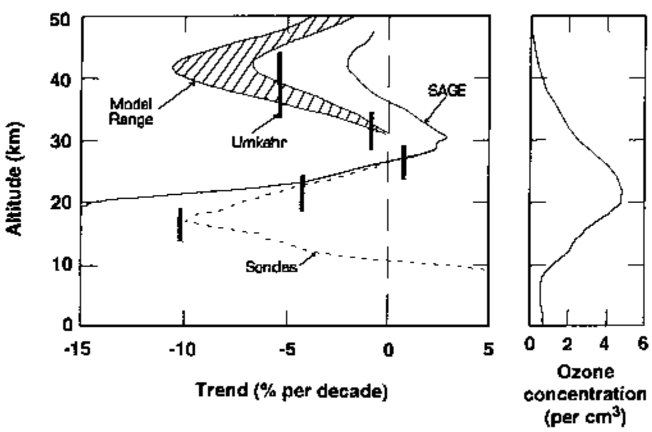

Summary

The Antarctic ozone hole of 1989 was deep and long-lasting and demonstrated that 1987 was not unusual. The 1990 ozone hole was also quite deep, similar to both 1987 and 1989. It lasted through December, the latest disappearance yet of the springtime ozone hole. The 1991 ozone hole was again deep and long-lasting and similar to that in 1989. Thus, 4 of the last 5 years have had deep long-lasting ozone holes. The previously noted quasi-biennial modulation of the severity of the ozone hole did not occur during the last 3 years. The area of the ozone hole has remained constant for the 4 years 1987, 1989, 1990, and 1991.

Statistically significant decreases in total ozone are now being observed in all seasons in both the Northern and Southern hemispheres at middle and high latitudes. Southern mid-latitude total ozone trends from the TOMS data are statistically significant in all seasons south of about 25°S. This is consistent with the analyses from the few Dobson stations with long records. The northern mid-latitude winter decrease found by the Ozone Trends Panel has continued, is now somewhat larger than previously reported, and has extended into the spring and summer. Most of the Dobson stations now show a statistically significant summer trend since 1970. The Dobson measurements have now been confirmed by independent measurement systems, that is, TOMS and SAGE. The decrease in total ozone amounts from the TOMS data is about 1% greater than those from the Dobson instruments at the same latitude. There is longitudinal structure to the trends derived from TOMS for northern mid-latitudes. The longitudinal structure in the Dobson data is less clear but reasonably consistent with that from TOMS. No statistically significant decreases are seen in tropical latitudes, from 25°S to 25°N.

SAGE and ozonesonde measurements have demonstrated that the decline in ozone concentration at northern middle latitudes is occurring primarily in the lower stratosphere. The declines in the lower stratosphere, below 25 km, are about 10% per decade, consistent with the observed decrease in column ozone. The measured upper stratospheric trends from both SAGE and Umkehr have a shape with altitude that is similar to model predictions, but the magnitude is somewhat smaller than that of the models. Tropospheric ozone increases of 10% per decade or more over the last two decades are seen over the few existing ozone sounding stations at northern middle latitudes.

REFERENCES AND NOTES

1. Depletion of stratospheric ozone due to the catalytic effect of NO_x emitted from a proposed fleet of supersonic transports was first predicted by H. Johnston [*Science* **173**, 517 (1971)]. The effects of chlorine from chlorofluorocarbons were predicted by M. J. Molina and F. S. Rowland [*Nature* **249**, 810 (1974)]. Subsequent progress in understanding has been reviewed in numerous papers and reports; see (*15*).
2. J. C. Farman, B. G. Gardiner, J. D. Shanklin, *Nature* **315**, 207 (1985).
3. For example, S. Solomon, *Rev. Geophys.* **26**, 131 (1988).
4. R. D. Bojkov, L. Bishop, W. J. Hill, G. C. Reinsel, G. C. Tiao, *J. Geophys. Res.* **95**, 9785 (1990); R. S. Stolarski, P. Bloomfield, R. D. McPeters, J. R. Herman, *Geophys. Res. Lett.* **18**, 1015 (1991).
5. R. Stolarski *et al.*, in "Scientific Assessment of Ozone Depletion: 1991" (World Meteorological Organization/United Nations Environment Program Report, World Meteorological Organization, Geneva, Switzerland, in press), chap. 2. The chapter was prepared with additional contributions from M. L. Chauin, V. Fioletev, S. Godin, V. Kirchhoff, W. Chu, J. DeLuisi, A. Hansson, J. Kerr, E. Lysenko, M. P. McCormick, P. Newman, M. Prendez, J. Staehelin, and B. Subbaraya.
6. G. M. B. Dobson, *Annals of the International Geophysical Year V, Part 1* (Pergamon, New York, 1957), pp. 46–89.
7. The network of Dobson observing stations, organized by the World Meteorological Organization and called the Global O_3 Observing System (GO_3OS), currently consists of about 70 stations. We use the 39 stations that have continuous records for approximately 30 years.
8. W. D. Komhyr, R. D. Grass, R. K. Leonard, *J. Geophys. Res.* **94**, 9847 (1989).
9. Ozone Data for the World (Atmospheric Environment Service, Department of the Environment, Downsview, Ontario, Canada, in cooperation with the World Meteorological Organization).
10. "Report of the International Ozone Trends Panel: 1988" (*World Meteorological Organization Global Ozone Research and Monitoring Network Report No. 18*, World Meteorological Organization, Geneva, Switzerland, 1990).
11. R. D. Bojkov, L. Bishop, W. J. Hill, G. C. Reinsel, G. C. Tiao, *J. Geophys. Res.* **95**, 9785 (1990).
12. R. D. Bojkov and V. Fioletev, in preparation.
13. A. J. Fleig, P. K. Bhartia, C. G. Wellemeyer, D. S. Silberstein, *Geophys. Res. Lett.* **13**, 1355 (1986).
14. J. R. Herman *et al.*, *J. Geophys. Res.* **96**, 7531 (1991).
15. "Scientific Assessment of Stratospheric Ozone: 1989" (*World Meteorological Organization, Global Ozone Research and Monitoring Project, Report No. 20*, World Meteorological Organization, Geneva, Switzerland, 1990).
16. W. D. Komhyr, *NOAA Tech. Mem. ERL ARL-149* (NOAA/GMCC, Boulder, CO, 1986).
17. R. D. Bojkov, in preparation.
18. J. Staehelin and W. Schmidt, *Atmos. Environ.* **25A**, 1739 (1991).
19. F. W. P. Götz, *Gerlands Beitr. Geophys.* **31**, 119 (1931).
20. C. L. Mateer and J. J. DeLuisi, in preparation.
21. J. J. DeLuisi, personal communication.
22. M. P. McCormick, J. M. Zawodny, R. E. Veiga, J. C. Larsen, P. H. Wang, *Planet. Space Sci.* **37**, 1567 (1989).
23. M. P. McCormick, R. E. Veiga, W. P. Chu, *Geophys. Res. Lett.* **19**, 269 (1992).
24. D. J. Hofmann, J. W. Harder, J. M. Rosen, J. V. Hereford, J. R. Carpenter, *J. Geophys. Res.* **94**, 16527 (1989); T. Deshler, D. J. Hofmann, J. V. Hereford, C. B. Sutter, *Geophys. Res. Lett.* **17**, 151 (1990); B. G. Gardiner, *ibid.* **15**, 901 (1988); W. D. Komhyr, R. D. Grass, R. K. Leonard, *J. Geophys. Res.* **94**, 11429 (1988).
25. R. S. Stolarski, M. R. Schoeberl, P. A. Newman, R. D. McPeters, A. J. Krueger, *Geophys. Res. Lett.* **17**, 1267 (1990); P. A. Newman, R. S. Stolarski, M. R. Schoeberl, R. D. McPeters, A. J. Krueger, *ibid.* **18**, 661 (1991).
26. A. J. Krueger, M. R. Schoeberl, P. A. Newman, R. S. Stolarski, in preparation.
27. R. R. Garcia and S. Solomon, *Geophys. Res. Lett.* **14**, 848 (1987); L. R. Lait, M. R. Schoeberl, P. A. Newman, *J. Geophys. Res.* **94**, 11559 (1989).
28. M. P. McCormick and J. C. Larsen, *Geophys. Res. Lett.* **13**, 1280 (1986); *ibid.* **15**, 907 (1988).
29. E. V. Browell *et al.*, *Polar Ozone Workshop* (*NASA Ref. Publ. 10014*, NASA, Greenbelt, MD, 1988), pp. 61–64.
30. M. H. Proffitt *et al.*, *J. Geophys. Res.* **94**, 16547 (1989).
31. G. C. Reinsel, G. Tiao, M. N. Wang, R. Lewis, D. Nychka, *Atmos. Environ.* **15**, 1569 (1981).
32. See, for example, G. C. Reinsel *et al.*, *J. Geophys. Res.* **92**, 2201 (1987).
33. R. D. McPeters and W. D. Komhyr, *ibid.* **96**, 2987 (1991).
34. R. S. Stolarski, P. Bloomfield, R. D. McPeters, J. R. Herman, *Geophys. Res. Lett.* **18**, 1015 (1991).
35. F. Lefevre and D. Cariolle, *ibid.*, p. 33; ______, S. Muller, F. Karcher, *J. Geophys. Res.* **96**, 12893 (1991); J. P. Pommereau, F. Goutail, H. LeTexier, T. S. Jorgensen, *Proceedings of the 28th International Astrophysical Colloquium*, Liège, Belgium, 1989.
36. H. U. Dütsch, J. Bader, and J. Staehelin (*J. Geomagn. Geoelectr.*, in press) reanalyzed the data from Payerne, Switzerland. R. D. Bojkov (in preparation) has reanalyzed the data from Churchill, Edmonton, and Goose Bay in Canada, Tateno in Japan, and Hohenpeissenberg in Germany.
37. R. E. Veiga and W. P. Chu, *Eos* **72**, 68 (1991).
38. P. Bloomfield, personal communication.